REFERENCE: ICF100809OR

IN SEARCH OF A PARAMETER FOR FRETTING FATIGUE

A. L. Hutson[2], T. Nicholas[1], S. Olson[2] and N. Ashbaugh[2]

[1]Air Force Research Laboratory, AFRL/MLLMN, Wright Patterson AFB, OH 45433, USA

[2] University of Dayton Research Institute, Dayton, OH 45469-0128, USA

ABSTRACT

Fretting fatigue experiments were conducted to determine the fatigue limit stress at 10^7 cycles for Ti-6Al-4V. A step-loading procedure was used to determine the fatigue limit stress that, in turn, was applied to the test geometry in numerical simulations using finite elements. Several fretting pad geometries and specimen thicknesses were used to obtain a range of normal and shear forces that produced the stress and displacement fields in the specimen. An evaluation was made of the conditions near the edge of contact where peak stresses occur to deduce parameters which lead to fretting fatigue failures at 10^7 cycles. However, no simple combination of stresses and slip displacements could be used to correlate all of the experimental data. A fracture mechanics methodology was also employed in order to determine the conditions for propagation or non-propagation of cracks that initiate in the edge of contact region. While no parameters were found which could uniquely predict the fretting fatigue failure, adjustment of the coefficient of friction based on computed slip displacements was shown to have a substantial effect on the stress and stress intensity factors. A correlation of friction coefficient with slip displacement is proposed as a possible method for consolidating data from fretting fatigue experiments conducted under different conditions.

KEYWORDS

fretting, fatigue, fracture mechanics, titanium

INTRODUCTION

Fretting fatigue is a type of damage occurring in the presence of contacts in which at least one of the components is subjected to bulk loading. It is normally associated with small magnitudes of relative slip, on the order of tens of microns, and little if any material removal and can lead to premature crack initiation and failure. Such damage has been indicated as the cause of many unanticipated disk and blade failures in turbine engines.

Under laboratory conditions, the synergistic effects of various parameters make determination and modeling of the mechanical behavior of fretting fatigue extremely difficult. The stress state in the contact region involves very high peak stresses, steep stress gradients, multi-axial stresses and differing mean stresses. Further, there is controversy whether the problem is primarily one of crack initiation or a crack propagation threshold, and whether or not stress states rather than surface conditions play a major role in the observed behavior. The parameters which govern the initiation and subsequent propagation of fretting fatigue cracks is still not well established. Thus the objectives of this investigation are to find several different fretting fatigue conditions analogous to the fatigue limit stress under uniaxial fatigue loading corresponding to a chosen high cycle fatigue (HCF) life. From these, both stress fields and stress intensity factors for specific cases can be obtained in order to find some commonality which may lead to development of parameters having broad application to fretting fatigue.

EXPERIMENTS

Tests were conducted using a high frequency test system to simulate the fretting fatigue loading conditions that occur in turbine engine blade attachments [1,2,3]. The apparatus uses flat fretting pads, with a radius at the edge of contact, against a flat specimen. Normal and shear loads are applied to the specimen as shown in Figure 1. A previous study has shown that the bending moment present in the apparatus is negligible relative to other parameters, and may be disregarded when designing the tests [4].

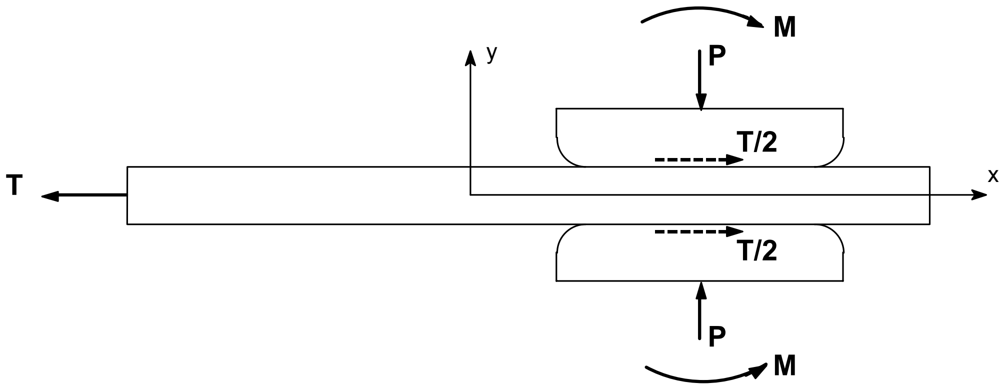

Figure 1: Test geometry and loading schematic.

The test geometry differs from conventional fretting fatigue tests [5,6] in two fundamental ways. First, the axial stress is transferred entirely to the fixture through shear. Resulting stresses in the specimen are zero on one end of the pad, thus the shear force into the pad is determined from the load applied to the specimen. Second, symmetry of the apparatus provides a specimen which breaks on one end, leaving the other end with a fretting scar and damage obtained under nominally identical conditions. As with a conventional fretting fatigue apparatus, the clamping force is constant and only the axial and shear loads are oscillatory.

All tests were conducted at 300 Hz under ambient lab conditions. Specimens and pads were taken from forged Ti-6Al-4V plates used in a series of investigations under a U.S. Air Force sponsored high cycle fatigue program. The processing and microstructure are reviewed in previous work [7,8]. Each specimen was subjected to uniaxial fatigue using a step-loading procedure [9] to determine a fatigue limit stress corresponding to 10^7 cycle fatigue life. Tests were conducted by incrementing the maximum axial stress by five percent of the initial value for various combinations of specimen thickness, pad length, and clamping force. The step loading technique was validated in earlier fretting fatigue studies using the same apparatus [3,10], and is outlined in reference [11].

ANALYSIS

Finite element analysis (FEA) results from a prior investigation [1] and additional computation provided stress fields through the specimen thickness and along the length of the specimen in the vicinity of the edge of contact. Load conditions were selected to cover a range of combinations of pad and specimen geometry, which produce average shear stresses typical of those tested in the experimental portion of the study. Conditions used in the numerical analysis are summarized in Table 1 along with some of the results for comparison. Axial stresses applied to the specimens in the model were taken from experimental observations. The model included pads with a 3.175 mm blending radius at both ends, resulting in an undeformed contact length of 6.35 mm for the short pad and 19.05 mm for the long pad. In two of the three test conditions simulated numerically [1,3,4], the coefficient of friction, μ, was taken as 0.3. The third case was run with μ=1.0, to allow comparison of results where only μ was changed.

Assuming cracks normal to the specimen surface under pure mode I loading, and using the stresses from the FEA, the stress intensity factor, K, was computed as a function of crack length. The K distributions were calculated using a program developed to model a single edge tension (SE(T)) specimen geometry under a non-constant σ_x stress field [12]. Some success has been reported in modeling fretting fatigue behavior as an edge notch, since both conditions produce similar stress fields [13]. Characterization results from a prior investigation [4] indicated that cracks nucleated at or near the edges of contact in specimens tested in the existing apparatus. The objective of these calculations was to compare the K values from two different cases where the peak stresses were significantly different, yet the stress fields both matched conditions corresponding to failure in 10^7 cycles.

The K solution program required material and crack dimension input parameters in addition to the stress distribution data. 120 GPa was used for the material modulus. The depth position of the final stress value given in the stress distribution, which was equal to half of the specimen thickness, was used for the final crack length. Stress intensity values are only reported for the first 100μm into the specimen thickness, although calculations were performed as far into the model specimen as possible using the available stress data from the FEA simulation.

TABLE 1

SUMMARY OF TEST CONDITIONS AND RESULTS FOR FINITE ELEMENT ANALYSIS.

Specimen thickness (mm)	Pad length (mm)	μ	Clamping Load (kN)	Applied σ_{axial} (MPa)	Average σ_y (MPa)	Average τ_{xy} (MPa)	Peak σ_x (MPa)	Max. Relative Displacement (μm)
1	12.7	0.3	49	275	770	21.6	1300	4.0
4	25.4	0.3	34	275	140	28.9	540	19.0
4	25.4	1.0	34	275	140	28.9	1100	3.4

RESULTS & DISCUSSION

The first results presented are the Haigh stresses corresponding to a 10^7 cycle fatigue life for the 1 mm and 4 mm thick specimens over a range of contact conditions (Figs. 2 and 3). The data are presented as a function of average applied clamping stress, which is taken to be positive. Two contact radii (CR) and two stress ratios are represented, and the baseline uniaxial fatigue limits for this material: 660 MPa @ R=0.5, 558 MPa @ R=0.1, are included. The numerical simulation conditions area also noted.

Much of the data for the 4 mm thick specimens was reported earlier [1] and seemed to indicate no appreciable trend as a function of applied clamping stress. However, the data for the 1 mm thick specimens do show a trend of increasing fatigue strength with decreasing applied clamping stresses, which was not noted in previous investigations [1,4]. The trend is not marked and conducting tests with clamping stresses much below 100 MPa to verify the trend is not possible, since clamping stress has to be applied to keep the specimen from pulling out of the grips in the current test apparatus. Also, the trend is obscured by experimental scatter in tests involving the smaller (0.4 mm) contact radius. Another feature to note in comparing Figures 2 and 3 is an apparent effect of thickness. The 4 mm thick specimens produced much lower fatigue limit stresses than 1 mm thick specimens under similar contact conditions, emphasizing the need for investigators to consider test specimen geometry issues closely in the development of life prediction models for service components.

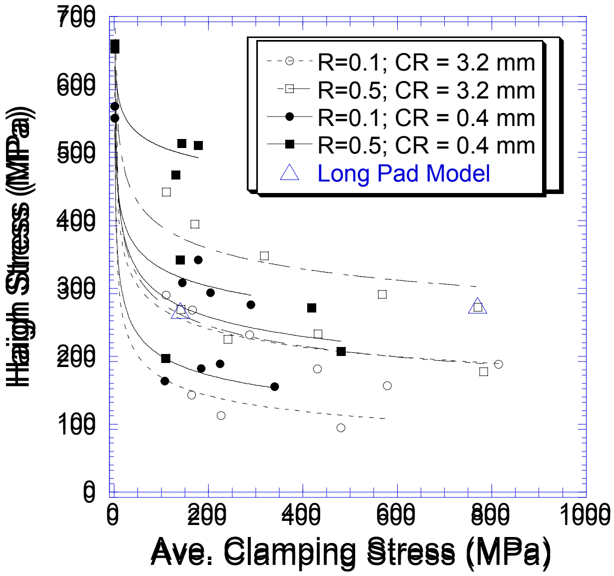

Figure 2: Experimental results for 1 mm thick specimens and unfretted baseline conditions.

Figure 3: Experimental results for 4 mm thick specimens and unfretted baseline conditions.

The next results presented are the K solutions plotted as a function of depth into the specimen (Figs. 4 through 6) for the deformed edge of contact (DEC) location and two adjacent locations 20 μm on either side of the DEC. In Figures 4, 5, and 6, y=0 corresponds to the surface of the specimen in contact with the pad. Each plot also includes the axial stress σ_x, illustrating the extent of the gradients into the specimen thickness for the corresponding K curve. The K values peak at the DEC, as do the stresses on the specimen surface. Other cases (not shown) for locations farther beyond the DEC indicated K values decaying proportional to the stress field. However, K distribution trends at the DEC show a continuous increase in K with crack length, and point to crack propagation to failure and not crack arrest, as reported for other geometries [5].

In comparing the various cases modeled here, we first address the cases where μ is taken as 0.3, a value which represents an average of values corresponding to gross slip over the entire pad length [1]. Data for the 1 mm thick specimen and short pad case are shown in Figure 5; data for the 4 mm thick specimen and long pad are shown in Figure 6. The values of maximum σ_x, shown in Table 1, vary from ~500 MPa for the 4 mm thick long pad case (Fig. 5) to ~1300 MPa for the 1 mm thick short pad case (Fig. 4). Since K depends strongly on the stress field, the calculated K values are higher for the case with the higher stresses, namely the 1 mm thick specimen and short pad case. Variations of stress gradients into the depth from one case to another are not too great and have little effect on the nature of the variation of K with crack length.

The experimental results for these two cases indicate nearly identical fatigue limits (Figs. 2 and 3). One would expect similar peak stresses and stress intensity factors in cases reflecting similar fatigue limits for the same fatigue life. As reported previously [1], differences in applied shear stress and average applied clamping stress at the contact for these two cases do not adequately explain the marked differences in the stresses from the numerical simulations. One possible explanation lies in the value of μ used in the analyses. Work by other researchers has indicated pronounced changes in μ over time under fretting fatigue conditions [14, 15], and as our previous work indicated, overall fretting fatigue behavior is extremely sensitive to μ.

Another observation from the previous work [1] was that the maximum relative displacement (see Table 1) at the edge of contact was considerably different for the two cases studied. This observation, coupled with the observation that increasing the value of μ resulting in increasing values of σ_x, lead to consideration of increasing μ for the case of the 4 mm thick specimen, which showed both lower stresses and higher relative displacements. While there is no physical basis for this assumption, the concept of higher μ for higher slip displacements is not totally without merit. It is also of interest to note that an early fretting parameter [10] contained the product of the stress and relative displacement. Perhaps the theory proposed here has the same

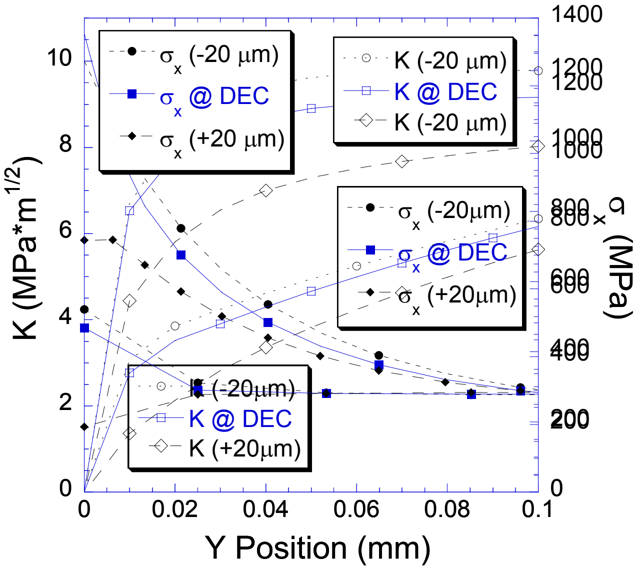

Figure 4: Stress distribution and resulting K solution for 1 mm thick specimen case.

Figure 5: Stress distribution and resulting K solution for 4 mm thick specimen, μ=0.3 case.

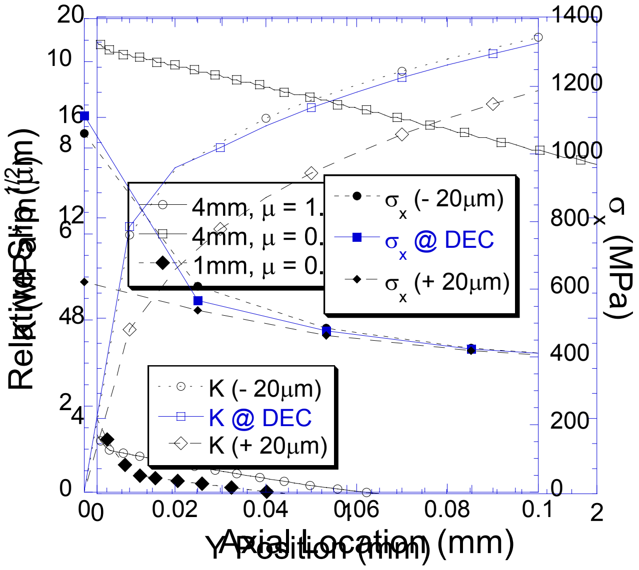

Figure 6: Stress distribution and resulting K solution for 4 mm thick specimen, μ=1.0 case.

Figure 7: Comparison of relative displacements along the contact calculated for all three simulation conditions identified in Table 1.

effect by increasing the stress through an increase in μ rather than through multiplying by relative displacement. To explore this concept the next comparison is of the two cases in which a 4 mm thick specimen with a long pad was modeled with two different values of μ. Increasing μ arbitrarily from 0.3 to 1.0 results in an increase in the maximum σ_x from ~ 500 MPa (Fig. 5) to 1100 MPa (Fig. 6). A similar increase was noted in the previous investigation of a 2 mm thick specimen [1]. Corresponding increases in maximum shear stresses were also noted for increases in μ, which are not discussed here. As with the previous comparison, the case with μ=1.0 resulting in higher tensile stresses also produced higher K values.

Changes in μ also produce changes in relative slip between the pad and specimen. In Figure 7, relative slip is plotted from the DEC, denoted by x=0, to x=2.0 mm under the fretting pad. Maximum slip distance occurs at the edge of contact, which is where the maximum tensile stresses occur. For the 4 mm thick specimen and long pad cases discussed above, the maximum slip distances corresponding to maximum tensile stresses is reduced from 19 μm (500 MPa) to 3.4 μm (1100 MPa). By comparison, the 1 mm thick specimen and short pad case produced a maximum relative slip of 4.0 μm (1300 MPa). These results are consistent with findings from the previous investigation, which concluded that stresses and displacements near the edge of contact are very sensitive to the value of μ between pad and specimen [1].

For the conditions modeled here, we hypothesized that initial slip conditions corresponding to μ=0.3 change over time to conditions of increasing μ, and thus increasing σ_x and corresponding K values. As shown above, higher tensile stresses and the resulting K values may be produced either by imposing a high clamping stress or by increasing μ. An equilibrium condition may exist for μ, which is dependent on the resultant relative displacement. If such a condition exists, an iterative method would be required to determine the final condition.

COMMENTS & CONCLUSIONS

Changes in μ over time for various fretting fatigue conditions vastly compound the problem of accurate life prediction for fretting fatigue, since it is very difficult to determine how μ will change over time. Further, such a change will be different for each combination of pad material, specimen material, applied loads, surface modification, and environment. Since fretting fatigue behavior is so profoundly influenced by μ which, in turn, may depend on relative displacements, additional research in how μ changes under fretting fatigue conditions is recommended.

Within the constraints of the geometry and test configuration and loading conditions examined in this investigation and under the assumptions made in the analyses, particularly that of μ being 0.3, the following conclusions can be drawn.

1. High levels of slip may produce increases in μ, which might have to be revised to produce higher stresses and smaller displacements.
2. Stress and relative displacement (slip) fields are very sensitive to the value of μ chosen for analysis.
3. Under the assumption of a Mode I crack normal to the surface, if a crack nucleates, it will continue to propagate to failure.

REFERENCES

1. Hutson, A.L., Nicholas, T., Olson, S.E., and Ashbaugh, N.E. *Submitted to Int. J. Fatigue.*
2. *Fretting Fatigue: Current Technologies and Practices, ASTM STP 1367*(1999). D.W. Hoeppner, V. Chandrasekaran, and C.B. Elliot (Eds). American Society for Testing and Materials, West Conshohocken, PA.
3. Hutson, A., Nicholas, T., and Goodman, R.(1999) *Int. J. Fat.* 21, 7, 663.
4. Hutson, A.L.(2000). MSc Thesis, University of Dayton, USA.
5. *Fretting Fatigue, ESIS 18*(1994). R.B. Waterhouse and T.C. Lindley (Eds). Mechanical Engineering Publications, London.
6. *Standardization of Fretting Fatigue Test Methods and Equipment, ASTM STP 1159*(1992). M. Helmi Attia, and R. B. Waterhouse (Eds). American Society for Testing and Materials, Philadelphia.
7. Peters, J.O. and Ritchie, R.O., *Submitted to Int. J. Fat*.
8. Moshier, M.A., Nicholas, T. and Hillberry, B.M., *Submitted to Int. J. Fat*.
9. Maxwell, D., and Nicholas, T.(1999). In: *Fatigue and Fracture Mechanics: 29th Vol., ASTM STP 1321,* pp. 626-641, T. L. Panotin and S. D. Sheppard (Eds), American Society for Testing and Materials, West Conshohocken, PA.
10. Ruiz, C., Boddington, P. H. B., and Chen, K. C.(1984) *Experimental Mechanics* 24, 208.
11. Thompson, S.R., Ruschau, J.J. and Nicholas, T. *Submitted to Int. J. Fat*.
12. John, R., Weight Function Analysis for a Single Edge Cracked Specimen, Unpublished work, Air Force Research Laboratory (AFRL/MLLN), Wright-Patterson AFB, OH.
13. Giannakopoulos, A.E., Lindley, T.C., Suresh, S., and Chenut, C. *Submitted to Fat. Frac. Eng. Mat. Structures.*
14. Szolwinski, M.P.. Matlik, S.F. and Farris, T.N.(1999). *Int. J. Fat.* 21, 671.
15. Farris, T.N., Harish, G., McVeigh, P.A., and Murthy, H.(2000). In: Proc of the 5th National Turbine Engine High Cycle Fatigue (HCF) Conference on CD, Session 13, Chandler, AZ.